

Complex Spike Activity of Purkinje Cells in the Ventral Uvula and Nodulus of Pigeons in Response to Translational Optic Flow

DOUGLAS R. W. WYLIE¹ AND BARRIE J. FROST²

¹Department of Psychology, University of Alberta, Edmonton, Alberta T6G 2E9; and ²Department of Psychology, Queen's University, Kingston, Ontario K7L 3N6, Canada

Wylie, Douglas R. W. and Barrie J. Frost. Complex spike activity of Purkinje cells in the ventral uvula and nodulus of pigeons in response to translational optic flow. *J. Neurophysiol.* 81: 256–266, 1999. The complex spike (CS) activity of Purkinje cells in the ventral uvula and nodulus of the vestibulocerebellum was recorded from anesthetized pigeons in response to translational optic flow. Translational optic flow was produced using a “translator” projector: a mechanical device that projected a translational optic flowfield onto the walls, ceiling, and floor of the room and encompassed the entire binocular visual field. CS activity was broadly tuned but maximally modulated in response to translational optic flow along a “best” axis. Each neuron was assigned a vector representing the direction in which the animal would need to translate to produce the optic flowfield that resulted in maximal excitation. The vector is described with reference to a standard right-handed coordinate system, where the vectors, $+x$, $+y$, and $+z$ represent, rightward, upward, and forward translation of the animal, respectively. Neurons could be grouped into four response types based on the vector of maximal excitation. $+y$ neurons were modulated maximally in response to a translational optic flowfield that results from self-motion upward along the vertical (y) axis. $-y$ neurons also responded best to translational optic flow along the vertical axis but showed the opposite direction preference. The two remaining groups responded best to translational optic flow along horizontal axes: $-x + z$ neurons and $-x - z$ neurons. In summary, our results suggest that the olivocerebellar system dedicated to the analysis of translational optic flow is organized according to a reference frame consisting of three approximately orthogonal axes: the vertical axis, and two horizontal axes oriented 45° to either side the midline. Previous research has shown that the rotational optic flow system, the eye muscles, the vestibular semicircular canals and the postural control system all share a similar spatial frame of reference.

INTRODUCTION

As an observer moves through the environment, proprioceptive feedback is provided by many sensory systems including the vestibular system, muscle senses, somatosensory system, and the visual system. That vision can act as a proprioceptive sense was emphasized by Gibson (1954), who noted that because the environment contains numerous stationary objects and surfaces, self-motion induces distinctive patterns of visual motion across the entire retina. Gibson (1954) called these patterns “optic flow” or “flowfields.”

The costs of publication of this article were defrayed in part by the payment of page charges. The article must therefore be hereby marked “advertisement” in accordance with 18 U.S.C. Section 1734 solely to indicate this fact.

In its simplest form, one can describe the motion of any object through space, including the self-motion of organisms, with reference to six degrees of freedom: rotation about three orthogonal axes, and translation along those axes (see Fig. 1A). Previous research has shown that the complex spike (CS) activity of Purkinje cells in the vestibulocerebellum (VbC) of pigeons is modulated in response to particular patterns of optic flow (Wylie and Frost 1991, 1993; Wylie et al. 1993). Neurons in the flocculus of the VbC respond best to rotational flowfields, whereas neurons in the ventral uvula and nodulus respond to translational flowfields (Wylie et al. 1993).

It originally was shown in rabbits by Simpson et al. (1981) that the neural system responsive to rotational optic flow is organized with respect to a reference frame consisting of three orthogonal axes (see also Graf et al. 1988; Leonard et al. 1988; Wylie and Frost 1993). Flocculus Purkinje cells respond best to rotation about either the vertical axis, or one of two horizontal axes oriented 45° to the midline. These studies were performed with the use of a “planetarium projector,” which projected rotational flowfields onto the walls, ceiling, and floor of the room. In this report, we further investigated the Purkinje cells in the ventral uvula and nodulus. Flowfield stimuli were produced with a “translator” projector, which is similar to the “planetarium” projector designed by Simpson and colleagues but critically different in that it presented translational rather than rotational flowfields. A preliminary report of this research has been published (Wylie et al. 1998).

METHODS

Surgery

The methods reported herein conformed to the guidelines established by the Canadian Council on Animal Care and were approved by the Biosciences Animal Care and Policy Committee at the University of Alberta. Silver King Pigeons were anesthetized with a ketamine (90 mg/kg)-xylazine (15 mg/kg) mixture (intramuscularly), and supplemental doses were administered as necessary. The animals were placed in a stereotaxic device with pigeon ear bars and beak adapter so that the orientation of the skull conformed with the atlas of Karten and Hodos (1967). A section of bone and dura on the left side of the head were removed to expose the auricle (flocculus) of the cerebellum.

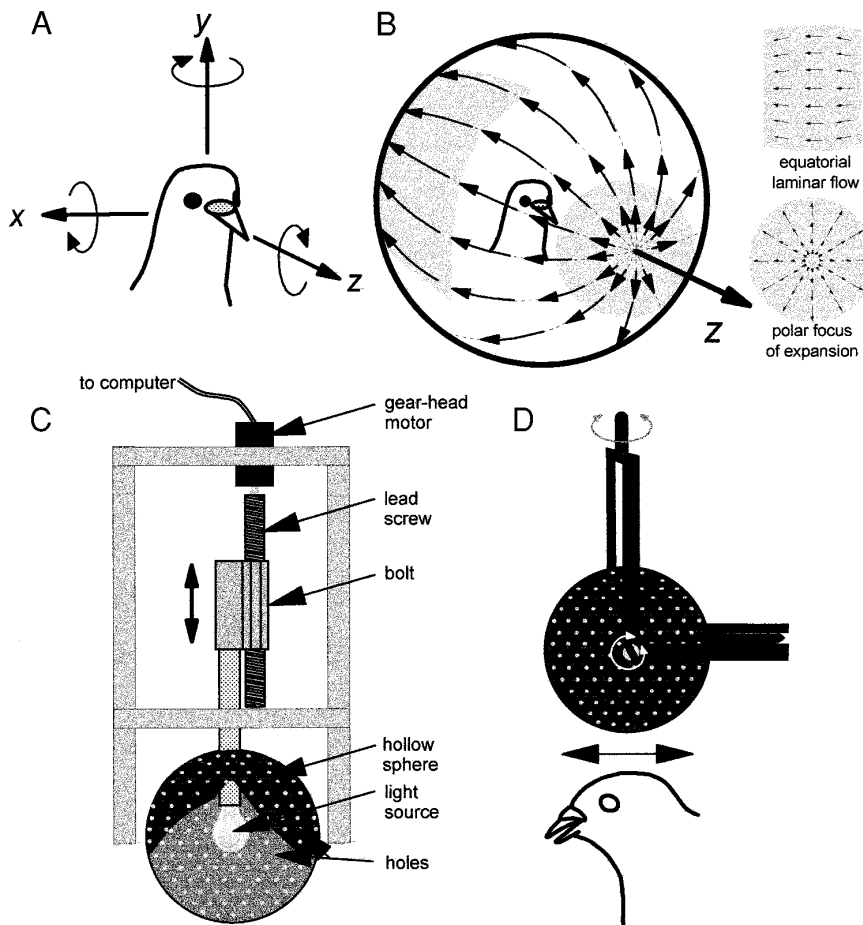


FIG. 1. *A*: generic description for motion of an object in 3-dimensional space using a standard coordinate system. It is sufficient to describe motion using a reference frame consisting of 3 orthogonal axes (x , y , z), and 6 degrees of freedom, 3 of translation, and 3 of rotation. With respect to translation, $+x$, $+y$, and $+z$ represent rightward, upward, and forward self-motion, respectively. *B*: schematic of the optic flowfield resulting from translation along the $+z$ axis. Arrows, as projected onto a sphere, represent the directions of local image motion in the visual flowfield. Shaded insets highlight the differences in local image motion at the "poles" and "equator" of the translational flowfield. At the pole in the direction of translation, the arrows diverge from a point; the focus of expansion (FOE). Likewise, at the opposite pole (not shown) the vectors would converge to a point; the focus of contraction (FOC). At the equators of the sphere, the flowfield is laminar, with all vectors pointing in approximately the same direction. *C*: translator used to produce translational flowfields. Translator consisted of a hollow sphere ~ 9 cm in diameter, the surface of which was pierced with numerous small holes. Part of the sphere has been cut away to reveal the light source within, which cast a field of dots onto the walls, ceiling, and floor of the darkened room. A gear-head motor, under computer control, drove a lead screw which moved the light source within the sphere. This effectively produced a translatory flowfield like that illustrated in *B*. As depicted in *D*, the translator was suspended above the animals head and mounted in gimbals such that the axis of translation could be positioned to any orientation within 3-dimensional space.

Extracellular recordings and optic flow stimulation

Extracellular recordings were made with glass micropipettes filled with 2 M NaCl and having tip diameters of $3\text{--}5\ \mu\text{m}$. To access the translation-sensitive cells in the ventral uvula and nodulus, the electrode was oriented 45° to the sagittal plane and advanced through the flocculus using an hydraulic microdrive (Frederick Haer). Extracellular signals were amplified, filtered, and fed to a window discriminator, which produced standard transistor transistor logic (TTL) pulses, each representing a single spike time. We recorded the complex spike (CS) activity of Purkinje cells in folium X (nodulus), and the ventral lamella of folium IXc, d (ventral uvula).

Once a cell was isolated, it was first stimulated with a large ($\sim 90 \times 90^\circ$) hand-held stimulus consisting of a random pattern of dots and lines. This was moved in various directions across the central zone of the visual field near the visual axis separately for each eye. With this type of stimulation, rotation-sensitive cells prefer opposite directions of motion in the central areas of both hemifields (Wylie et al. 1993). Rotation-sensitive cells were not studied further as we previously have described their responses to optic flow produced by a planetarium projector (Wylie and Frost 1993). Translation-sensitive cells, which we have previously characterized as preferring the same direction of motion in the central regions of both hemifields (Wylie and Frost 1991; Wylie et al. 1993), were further studied with a translator projector. The translator, illustrated in Fig. 1C, consisted of a small, hollow metal sphere (diameter = 9 cm), the surface of which was drilled with numerous small holes. A small filament light source was moved along a segment of a diameter

path within the sphere (under computer control), so that a moving pattern of light dots was projected onto the walls, ceiling, and floor of the room. This pattern essentially covered the entire binocular visual field. Movement of the light source inside the stationary sphere produced a translational flowfield, with a focus of expansion (FOE) at one "pole," a focus of contraction (FOC) at the opposite "pole," and laminar flow at the "equator" (see Fig. 1B). By mounting the "translator" in gimbals, the axis of the spherical translational flowfield could be positioned to any orientation within three-dimensional space (see Fig. 1D). The speed of the "equatorial" dots was $\sim 1\text{--}2^\circ/\text{s}$, and the dots were $\sim 1\text{--}2^\circ$ in diameter. Each sweep consisted of 5.3 s of motion in one direction along the axis of the translator, a 5.3-s pause, 5.3 s of translation in the opposite direction, and a 5.3-s pause. The start of each sweep was synchronized with the collection of TTL pulses from the window discriminator and peristimulus time histograms (PSTHs) were constructed using a CED 1401Plus and Spike2 for Windows software (Cambridge Electronic Designs). PSTHs were summed over 5–20 sweeps. Data were collected in response to translational optic flow along various axes in three dimensional space. Shown in Fig. 1A, we used the standard right-handed coordinate system where the x , y , and z axes represent leftward-rightward, upward-downward, and forward-backward motion, respectively. With respect to direction along these three axes, $+x$, $-x$, $+y$, $-y$, $+z$, and $-z$ represent rightward, leftward, upward, downward, forward, and backward translation respectively, and refer to motion of the animal. Cells were difficult to hold for long periods of time, but attempts were made to obtain data under binocular and monocular viewing conditions.

RESULTS

CS activity was recorded from 46 Purkinje cells in the ventral uvula and nodulus of 16 pigeons. The average spontaneous firing was 0.91 ± 0.11 (SE) spikes/s. Thirty-eight of these neurons had binocular receptive fields, exhibited direction-selectivity in response to movement of the hand-held target, and preferred the same direction of motion (in the central visual zones around the visual axes) in both hemifields. A cell was deemed direction selective if the ratio of the firing rate in response to a translational flowfield in the best direction versus the firing rate in response to translation in the opposite direction was ≥ 1.5 . For the 38 cells the average of this ratio was 4.7 ± 0.6 . Seven cells did not meet the criteria to be classified as directionally selective. One additional cell was directionally selective but had a monocular (contralateral) receptive field.

Stimulation with the translator revealed that the 38 cells

could be categorized into four groups based on the axis preference: $-x-z$ neurons, $-x+z$ neurons, $-y$ neurons, and $+y$ neurons.

 $-x-z$ neurons

Nine neurons were classified as $-x-z$ neurons. In response to the hand-held stimulus, these neurons preferred forward (temporal to nasal) visual motion in the central visual field of each eye. With the translator, these neurons responded best to a translational flowfield along a horizontal axis that was oriented at 45° contralateral (45°c) azimuth. The one cell that had a monocular-contralateral receptive field also could have been included in this group in that it showed the same axis preference as these nine neurons. Responses of a $-x-z$ neuron to translational optic flow along several axes is shown in Fig. 2. In *A* and *B*, an azimuthal tuning curve in

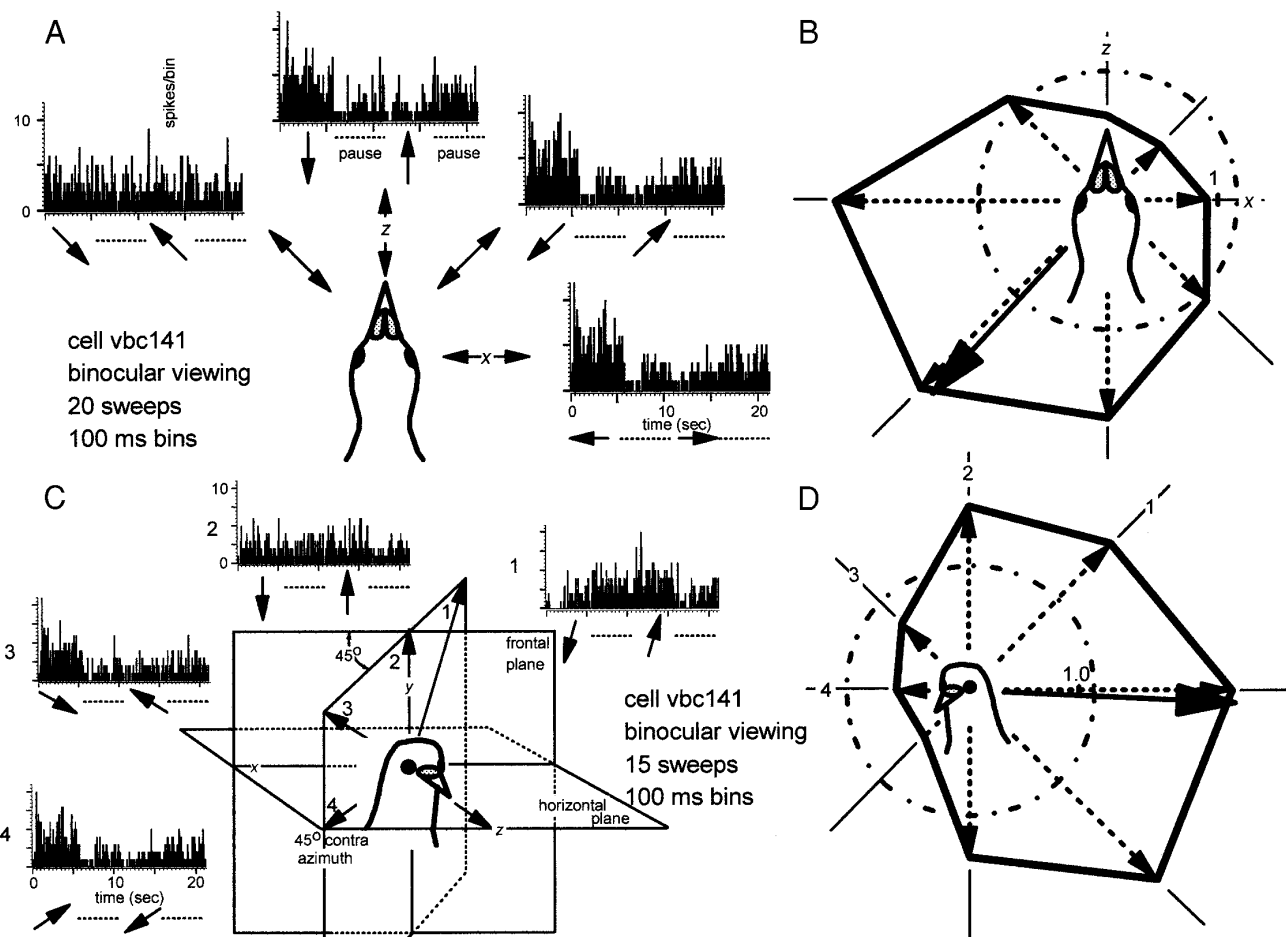
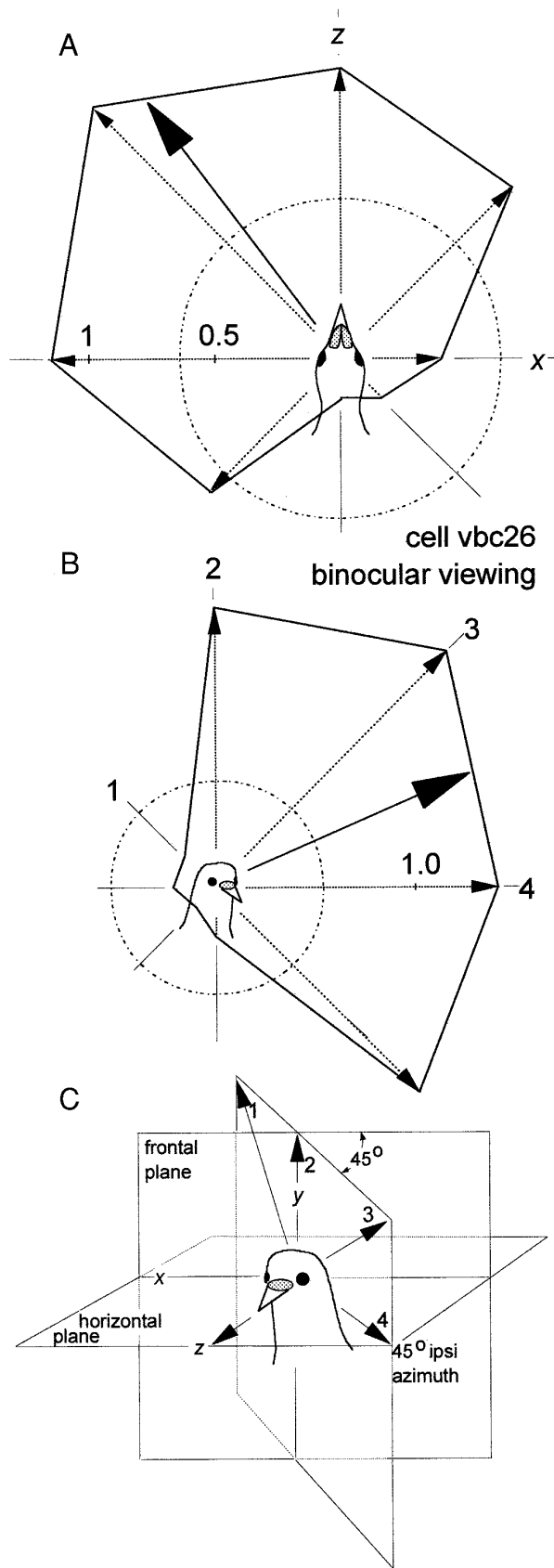


FIG. 2. Responses of a $-x-z$ neuron. In *A* and *B*, azimuthal tuning (in the horizontal plane) is shown, whereas in *C* and *D*, elevational tuning in a vertical plane that intersects the horizontal plane at 45° contralateral (45°c) azimuth is shown. In *A* and *C*, peristimulus time histograms (PSTHs) in response to translational optic flow along 4 axes are shown. For each sweep, there was 5.3-s translation in one direction, followed by a 5.3-s pause, 5.3-s translation in the opposite direction, and a 5.3-s pause. Arrowheads point to the FOE in the flowfield, i.e., the direction in which the animal would move to cause such a flowfield. *B* and *D*: polar plots [firing rate (spikes/s) as a function of the orientation of the axis of translational flow in polar coordinates] of the data from *A* and *C*, respectively. In the polar plots, the spontaneous firing rate is represented by broken circles; solid arrows, axes of maximal modulation from the best cosine fits. For clarity, corresponding axes in *C* and *D* are indicated by the numerals 1–4, where axis 2 is the y axis and axis 4 is an horizontal axis at 45°c azimuth. Note that this cell responded best to translational optic flow along the a horizontal axis oriented at 45°c azimuth, showing maximal excitation and inhibition in response to the negative and positive directions, respectively.



the horizontal plane is shown, whereas in *C* and *D*, elevation tuning is shown in a vertical plane that intersects the horizontal plane at 45° azimuth (i.e., the plane is normal to the vector $-x+z$). In *A* and *C*, PSTHs are shown in response to translational optic flow along each of the four axes. *B* and *D*, respectively, show polar plots of the data shown in *A* and *C*: firing rate is plotted as a function of the direction of translational optic flow, in polar coordinates, and the spontaneous firing rates are represented by the broken circles. In this and subsequent figures, the orientation of the arrows reflects the orientation of the axis of translational optic flow, and the arrowheads indicate the direction along the axis in which the animal would have to move to produce such a flowfield. That is, the arrowheads point to the FOE in each flowfield. In the polar plots, the solid arrows represents the vector of maximal excitation (“best axis”), which was calculated by fitting a cosine to the tuning curve and determining its peak. From Fig. 2 it is clear that, although broadly tuned, this neuron was modulated maximally by translational optic flow along the vector $-x-z$. That is, this neuron was maximally excited in response to a flowfield with a FOC at 45° azimuth [and a FOE at 135° ipsilateral (135°i) azimuth], and motion in the opposite direction resulted in strong inhibition. Little modulation occurred in response to translation along orthogonal axes [i.e., the “null” axes; the *y* axis (*B* and *D*) and the horizontal axis $-x+z$ (*A* and *C*)].

In Fig. 7*B* the best axes from azimuth tuning curves in the horizontal plane of all nine $-x-z$ neurons are shown. Note that the best axes cluster about the axis oriented at 135°i azimuth (mean \pm SE = 133.1 \pm 2.1°). Figure 4*A* also shows averaged data of the azimuth tuning curves of the nine $-x-z$ neurons but presented as a “mean normalized tuning curve.” To construct this tuning curve, for each $-x-z$ neuron, the firing rate in response to translational optic flow along each axis in the horizontal plane was expressed as a percentage of the cell’s maximal firing rate. This percentage then was averaged across all nine $-x-z$ neurons for each of the eight directions. The average firing rate firing (mean \pm SE) expressed as a percentage is plotted as a function of the direction of translational optic flow. The broken circle represents the average spontaneous rate, and the shaded ring represents ± 1 SE. The best axis calculated from the best cosine fit was 132.9°i azimuth (solid arrow).

Complete elevation tuning curves in the plane depicted in Fig. 2*C* were obtained for four $-x-z$ neurons, and the best axes are shown in Fig. 7*D*. The average of this distribution was approximately in the horizontal plane (mean \pm SE = +6.2 \pm 9.7° elevation). The mean normalized tuning curve in this plane for $-x-z$ neurons is shown in Fig. 4*B*. The

FIG. 3. Responses of a $-x+z$ neuron. Polar plots of azimuthal tuning in the horizontal plane (*A*) and elevation tuning in a vertical plane that intersects the horizontal plane at 45° ipsilateral (45°i) azimuth (*B*) are shown. This vertical plane is illustrated in *C*. Corresponding axes in *B* and *C* are indicated by the numerals 1–4, where axis 2 is the *y* axis and axis 4 is an horizontal axis at 45°i azimuth. In the polar plots, broken circles, spontaneous firing rate; solid arrows, axes of maximal modulation from the best cosine fits. Note that this cell responded best to translational optic flow along the a horizontal axis oriented at 45°i azimuth, showing maximal excitation and inhibition in response to the positive and negative directions, respectively. As *B* shows there was a +*y* component to the best axis.

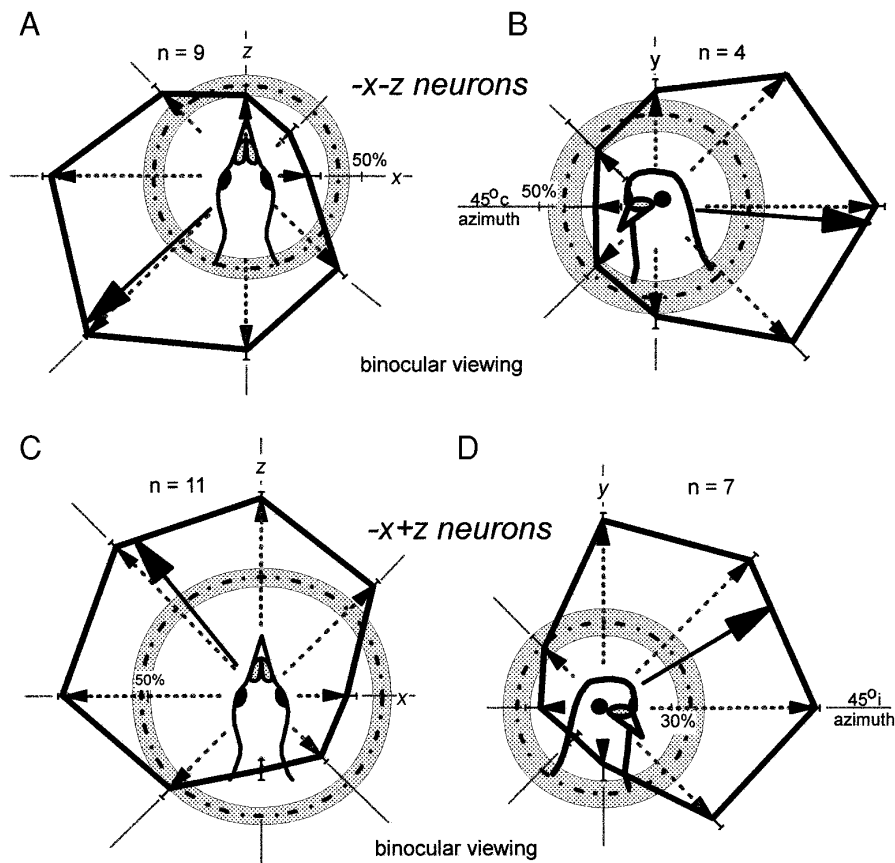


FIG. 4. Mean normalized tuning curves for $-x-z$ and $-x+z$ neurons. Azimuthal tuning is shown in the horizontal plane for both types of neurons (A and C). B: elevation tuning is shown for $-x-z$ neurons in the a vertical plane that intersects the horizontal plane at $45^\circ c$ azimuth. D: elevation tuning is shown for $-x+z$ neurons in the a vertical plane that intersects the horizontal plane at $45^\circ i$ azimuth. To construct the tuning curve shown in A (for example), for each $-x-z$ neuron the firing rate in response to translational optic flow along each axis in the horizontal plane was expressed as a percentage of the cell's maximal firing rate. Average response of the 9 $-x-z$ neurons to translational optic flow along each axis then was calculated. Average firing rate firing (mean \pm SE) expressed as a percentage is plotted as a function of the direction of translational optic flow. Broken circle, average spontaneous rate; shaded ring, ± 1 SE. Solid arrows represent the peaks of the best cosine fits.

best axis for this tuning curve was approximately horizontal (-1.9° elevation; solid arrow).

$-x+z$ neurons

Eleven neurons were classified as $-x+z$ neurons. With the hand-held stimulus, these neurons were characterized as preferring backward (nasal to temporal) visual motion around the center of the visual field of each eye. With the translator, these neurons responded best to a translational flowfield along a horizontal axis that was oriented at $45^\circ i$ azimuth. Responses of a $-x+z$ neuron are shown in Fig. 3. In Fig. 3A, the polar plot of an azimuth tuning curve in the horizontal plane is shown. This neuron was maximally excited in response to a flowfield along the vector $-x+z$ (i.e., a flowfield with a FOE at $45^\circ i$ azimuth and a FOC at $135^\circ c$ azimuth), and motion in the opposite direction resulted in strong inhibition. The best axes of the 11 $-x+z$ neurons are shown in Fig. 7B. Note the clustering of the vectors at $\sim 45^\circ i$ azimuth (mean \pm SE = $39.7 \pm 3.8^\circ i$ azimuth). A mean normalized azimuth tuning curve for the 11 $-x+z$ neurons is shown in Fig. 4B. The best axis was $38.0^\circ i$ azimuth.

Figure 3B shows a polar plot of the elevation tuning curve in the vertical plane that intersects the horizontal plane at $45^\circ i$ azimuth for the same $-x+z$ neuron shown in 3A. That is, the elevation tuning was in the plane normal to the vector $+x+y$ (depicted in Fig. 3C). Note that the best axis is not in the horizontal plane but has a $+y$ component. In fact, the

best axis was $+23^\circ$ elevation in this plane. Complete elevation tuning curves in this plane were obtained for seven $-x+z$ neurons, and the best axes are shown in Fig. 7C. Note that all seven of the best axes had a $+y$ component. The average of this distribution was $29.6 \pm 4.8^\circ$ (mean \pm SE) elevation. The mean normalized elevation tuning curve in this plane for $-x+z$ neurons is shown in Fig. 4D. The best axis was $+32.1^\circ$ elevation.

$-y$ neurons

Ten neurons were classified as $-y$ neurons. With the hand-held stimulus, these neurons preferred upward motion in both hemifields. In our previous studies we dubbed these "descent" neurons as they respond best to a flowfield that would result from the bird descending (Wylie and Frost 1991; Wylie et al. 1993). With the translator, these neurons showed maximal excitation in response to $-y$ translation, (i.e., a flowfield with the FOE below the animal), and $+y$ translation resulted in strong inhibition. Figure 5A shows the polar plot of an elevation tuning curve in the sagittal plane for a $-y$ neuron. The best axes of all 10 $-y$ neurons are shown in Fig. 7A. Note the clustering about the $-y$ axis (mean \pm SE = $-85.5 \pm 5.3^\circ$ elevation). A mean normalized elevation tuning curve in the sagittal plane for $-y$ neurons is shown in Fig. 5B. The best axis for this tuning curve was -84.3° elevation.

$+y$ neurons

Eight neurons were classified as $+y$ neurons. With the hand-held stimulus, these neurons preferred downward

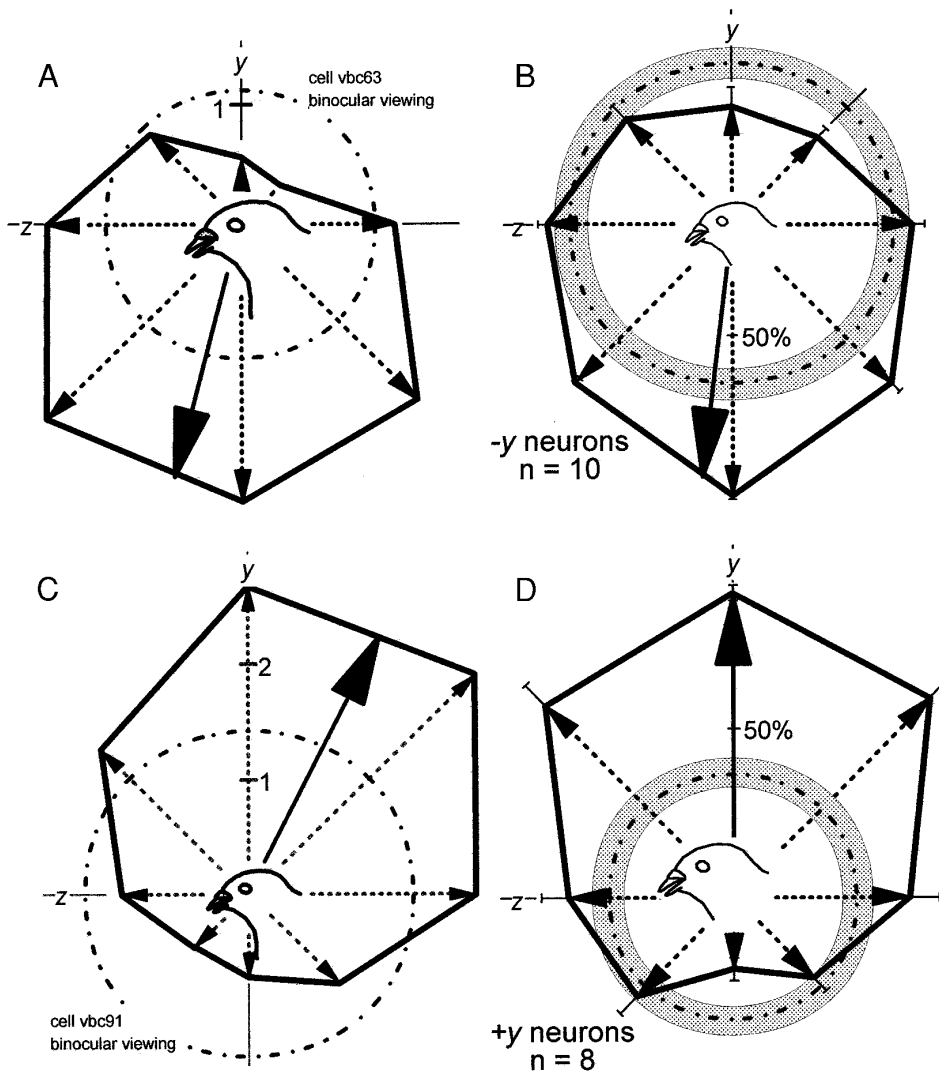


FIG. 5. Responses of $-y$ and $+y$ neurons. Elevation tuning curves in the sagittal plane for individual $-y$ (A) and $+y$ (C) neurons are shown. B and D: mean normalized elevation tuning curves for $-y$ and $+y$ neurons, respectively. Broken circles, spontaneous rate; shaded ring, ± 1 SE. Solid arrows represent the peak of the best cosine fits.

motion in the central zone around the visual axis in both hemifields. In our previous studies, we dubbed these ‘‘ascent’’ neurons as they respond best to a flowfield that would result from the bird ascending (Wylie and Frost 1991; Wylie et al. 1993). With the translator, these neurons responded best to a translational flowfield along the y axis but showed the opposite direction preference of $-y$ neurons. $+y$ translation (producing a flowfield with a FOE above the animal’s head) resulted in maximal excitation, and $-y$ translation resulted in strong inhibition. Figure 5C shows an elevation tuning curve in the sagittal plane for a $+y$ neuron. The best axes of all eight $+y$ neurons are shown in Fig. 7A. The average of this group was $91.1 \pm 9.6^\circ$ elevation (mean \pm SE). A mean normalized elevation tuning curve in the sagittal plane for $+z$ neurons is shown in Fig. 5D. The best axis of this tuning curve was 90.1° elevation.

Monocular versus binocular stimulation

With the hand-held target it was clear that all 38 cells responded to stimulation of both visual hemifields and pre-

ferred approximately the same direction of motion in central zones of each eye. However, quantitative tuning curve data in response to monocular stimulation were obtained from only nine cells. Using criteria we have used in previous studies (Wylie et al. 1993), three cells were classified as having no ocular dominance (OD), two cells showed a slight ipsilateral OD, two cells had a marked ipsilateral OD, one cell had a slight contralateral OD, and one cell was classified as having a marked contralateral OD. Figure 6 shows azimuthal tuning curves for an equidominant $-x+z$ neuron under contralateral (A) and ipsilateral (B) viewing conditions. The response of this cell to binocular stimulation is shown in Fig. 3. Comparing Figs. 3A and 6, A and B, it is apparent that the best axis was similar for both eyes under monocular viewing conditions and during binocular stimulation.

For six of the nine cells, in response to translational optic flow along the preferred axis, binocular stimulation resulted in a greater depth of modulation when compared with monocular stimulation of the dominant eye alone. For the other three cells, modulation in response to binocular stimulation was about the same as that in response to stimulation of the

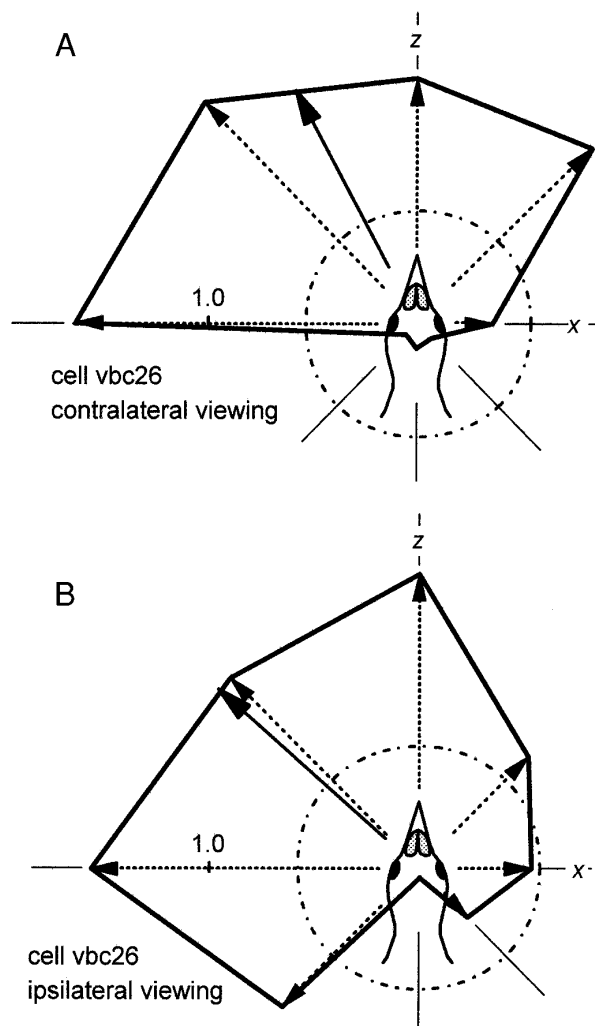


FIG. 6. Monocular azimuthal tuning curves for a $-x+z$ neuron. Azimuthal tuning (in the horizontal plane) is shown for the same neuron shown in Fig. 3, in response to stimulation of either the contralateral (A) or ipsilateral (B) visual field. Broken circles, spontaneous firing rate; solid arrows, axes of maximal modulation from the best cosine fits. Note that the best axes are approximately the same for ipsi- and contralateral stimulation.

dominant eye. For the nine cells inclusive, the average ratio of binocular to monocular modulation was 1.56 ± 0.22 (mean \pm SE).

Functional organization

In the course of our recordings it became clear that the four functional classes of translation sensitive neurons were found in discrete parasagittal zones, each ~ 0.5 mm wide, within the VbC. The most medial zone, (zone 1), was immediately adjacent to the midline and contained $-x-z$ neurons. Zones 2–4, contained $-x+z$, $-y$, and $+y$ neurons, respectively. These observations were confirmed in concurrent anatomic studies in which neural tracers were injected at the locations identified by CS responses to translational optic flow (Lau et al. 1998). Figure 8 shows the results of an experiment in which two penetrations were made in the same

coronal plane, and an injection of biotinylated dextran amine (see Lau et al. 1998) was made at one of the recording sites. Note that the rotation-sensitive cells were found laterally in the flocculus.

DISCUSSION

In this study, we recorded the CS activity of Purkinje cells in the ventral uvula and nodulus of pigeons in response to translational flowfields produced by a translator projector. This visual input arises from climbing fibers originating in the ventrolateral margin of the medial column (mc) of the inferior olive (IO) (Lau et al. 1998). The mc receives input from two retinal recipient nuclei, the pretectal nucleus lenticiformis mesencephali (LM) and the nucleus of the basal optic root (nBOR) (Fite et al. 1981; Gamlin and Cohen 1988; Karten et al. 1977; Reiner et al. 1979). Most LM and nBOR neurons have very large receptive fields without inhibitory surrounds and respond best to large field stimuli moving in contralateral visual field (Burns and Wallman 1981; Gioanni et al. 1984; Morgan and Frost 1981; Winterson and Brauth 1985; Wolf-Oberhollenzer and Kirschfeld 1994; Wylie and Frost 1990, 1996). In the companion paper (Wylie and Frost 1999), we describe the responses of a small subpopulation of nBOR neurons that have binocular receptive fields and respond best to either translational or rotational optic flow.

Common reference frame for self-translation and self-rotation

In the present study, we have shown that Purkinje cells in the ventral uvula and nodulus of the VbC respond best to translational optic flow along one of three approximately orthogonal axes: a vertical axis ($+y$ and $-y$ neurons) and two horizontal axes oriented 45° to the midline ($-x-z$ and $-x+z$ neurons). Previous studies have shown that floccular Purkinje cells respond best to rotational optic flow about one of two axes: either the vertical axis or a horizontal axis oriented at 45° contralateral azimuth (Graf and Simpson 1981; Graf et al. 1988; Simpson et al. 1981; Wylie and Frost 1993). Simpson, Graf, and colleagues (Ezure and Graf 1984; Graf et al. 1988; Leonard et al. 1988; Simpson and Graf 1981, 1985; Simpson et al. 1988a,b, 1989a,b; van der Steen et al. 1994; see also Wylie and Frost 1996) noted that the vestibular canals and the eye muscles share this same frame of reference. The horizontal canals are maximally sensitive to rotation about the vertical axis, whereas one anterior canal (and the contralateral coplanar posterior canal) responds best to rotation about a horizontal axis oriented at 45° azimuth. The horizontal recti, vertical recti, and oblique muscles rotate the eye about a vertical axis, a horizontal axis oriented at 135° azimuth, and a horizontal axis oriented at 45° azimuth, respectively. Together, these studies show that the sensory systems involved in analysis of self-rotation (i.e., the visual, vestibular systems) and the output of this system (i.e., the eye muscles which generate compensatory rotary eye movements) all share the same spatial frame

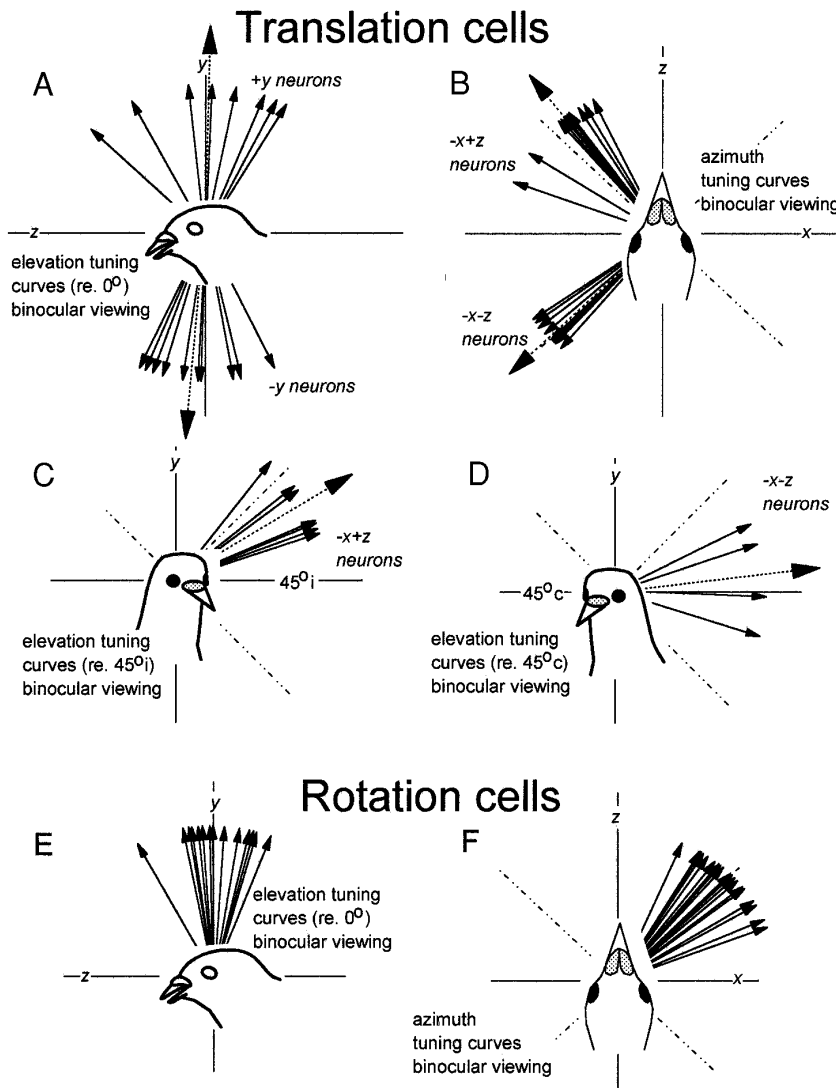


FIG. 7. Reference frames coding self-translation and self-rotation in the vestibulocerebellum. *A*: distribution of best axes of translation for $+y$ and $-y$ neurons. Each arrow represents the peak of the best cosine fit to the elevation tuning curves in the sagittal plane. *B*: distribution of the best axes of $-x+z$ and $-x-z$ neurons where each arrow represents the best cosine fit to azimuthal tuning curves in the horizontal plane. *C*: distribution of best axes for $-x+z$ neurons in elevation. Here the arrows denote the best axes of determined from elevation tuning curves in the vertical plane normal to the vector $x+z$. That is, this vertical plane intersects the vertical plane at 45° azimuth and is illustrated in Fig. 3*C*. Similarly, *D* shows the distribution of best axes for $-x-z$ neurons in elevation. Arrows denote the best axes determined from elevational tuning curves in the vertical plane normal to the vector $+x-z$. That is, this vertical plane intersects the horizontal plane at 45° azimuth and is illustrated in Fig. 2*C*. *A-D*: larger arrows with broken lines represent the means of the respective distributions. *E* and *F*: best axes of rotation-sensitive cells in the flocculus determined from elevational tuning curves in the sagittal plane and azimuthal tuning curves in the horizontal plane, respectively. Data in *E* and *F* are from Wylie and Frost (1993).

of reference. In Fig. 9*A*, we show available data from pigeons illustrating the correspondence of the reference frames of those systems dealing with self-rotation. Flocculus neurons sensitive to optic flow, the semicircular canals, and the eye muscles all share a common reference frame (Baldo 1990; Dickman 1996; Wylie and Frost 1993). Dickman (1996) recorded from primary afferents innervating the vertical canals and showed that they respond best to rotation about an horizontal axis oriented $\sim 45^\circ$ to the midline.

The results of the present study show that the visual system responsible for the analysis of translational optic flow also is organized with respect to the same three axis reference frame (Fig. 9*B*). Hess and Dieringer (1991) also have suggested that the otolith organs of the vestibular system, which are responsive to the linear accelerations produced by translation, also appear to be organized in semicircular canals coordinates. Moreover, neural systems controlling postural responses to translation may be organized similarly. In response to translation of the floor in different directions in the horizontal plane, Macpherson

(1988) found that forelimb and hindlimbs of cats were maximally responsive to displacement directions approximately 45° to the midline. However, the primary afferents innervating the utricle in pigeons do not share this coordinate system. Si et al. (1997) has shown that most utricular afferents in pigeons respond best to linear translation along the interaural (x) axis.

Optimal reference frame

Because optic flowfields are often complex, involving both translational and rotational components, we speculate that there is some computational advantage to a common spatial frame of reference. Simpson and Graf (1985) have argued that a reference frame consisting of a vertical axis and two horizontal axes oriented 45° to the midline is the most "economical" for the analysis of self-rotation. This is illustrated in Fig. 10, *A* and *B*, and in *C* and *D*, we show that the same argument can be made for the analysis of self-translation. *A* shows the idealized orientation of the vestibular

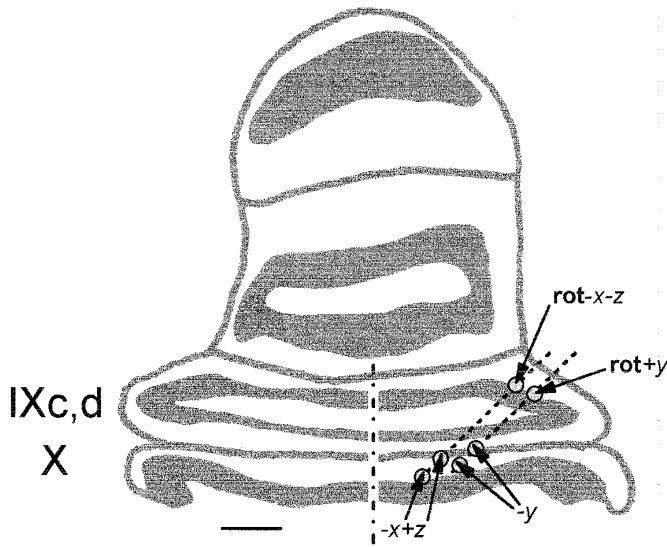


FIG. 8. Functional organization of the pigeon vestibulocerebellum (VbC). Two penetrations in the same coronal plane are indicated (---). Electrode was oriented 45° to the sagittal plane. Cells responsive to translation along horizontal axes were found medial to cells responsive to translation along the vertical axis. Cells responsive to rotation about the vertical axis (rot+y) or the -x-z axis (rot-x-z) were found laterally in the flocculus.

lar canals (as projected onto a horizontal plane) in vertebrates. They are bilaterally symmetrical, mutually orthogonal, and organized as a “push-pull” system. A leftward rotation of the head about the vertical axis excites afferents in the left horizontal canal and inhibits afferents in the right horizontal canal. A head rotation about the horizontal axis +x+z (in the direction indicated by the arrows), maximally excites the left anterior canal and inhibits the right posterior canal. *B* shows a system organized such that the cardinal axes are roll, pitch, and yaw. Although bilaterally symmetrical, three pairs of canals are insufficient in this configuration as a rotation about the y axis is not organized in a push-pull fashion. An extra pair of canals (black in the figure) would be necessary.

The results of the present study support a push-pull

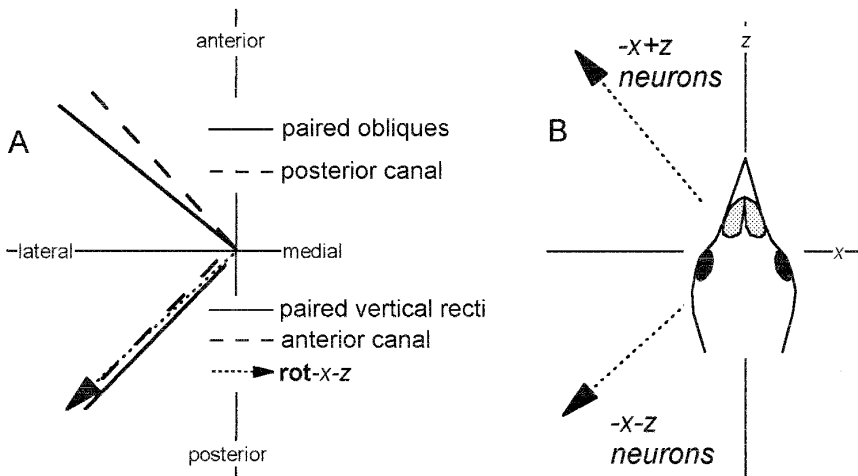


FIG. 9. Reference frames for optic flow, the vestibular canals and the eye muscles. *A*: preferred axes of the vertical semicircular canals (from Baldo 1990; but see Dickman 1996), the oblique muscles and vertical recti (measurements by Wylie and Frost 1996), and the average best axis of the VbC neurons responsive to rotational optic flow about the -x-z axis (rot-x-z Purkinje cells) (from Wylie and Frost 1993). *B*: average best axis for -x+z and -x-z neurons in response to translational optic flow from the present study. For all these systems, the best axes cluster at ~45° to the midline.

bilaterally symmetric reference frame depicted in Fig. 10C for the analysis of self-translation. Like the reference frame for self-rotation shown in *A*, this system consists of two horizontal axes oriented 45° to either side of the midline as shown in *C*. This is more economical than the arrangement shown in *D*, which has the *x* and *z* axes as principle axes: as in *B*, three horizontal axes would be required. Either way to satisfy the constraints of bilateral symmetry and a push-pull system, both +y and -y neurons would be needed on both sides of the brain. Thus for self-translation, the four-channel three-axes system we have shown in *C*, consisting of -x+z, -x-z, +y, and -y neurons, is more economical in satisfying the constraints of bilateral symmetry and a push-pull system than the arrangement shown in *D*.

Actually, the three principal axes of the translational optic flow system, as revealed in the present study, are not quite orthogonal. Although, on average, the best axes of -x-z neurons lie within the horizontal plane (Figs. 2, 4B, and 7D), the best axes of -x+z neurons are not within the horizontal plane but have a +y component (Figs. 3B, 4D, and 7C). However, these results are consistent with what is known about the direction preferences of accessory optic system neurons. Most neurons in the nBOR prefer upward, downward, or backward (N-T) whole-field motion in the contralateral eye (Wylie and Frost 1990), whereas most neurons in the LM prefer forward (T-N) whole-field motion in the contralateral eye (Winterson and Brauth 1985; Wylie and Frost 1996). We previously have emphasized that the direction preference of N-T nBOR neurons and T-N LM neurons are not colinear. For N-T neurons, the average direction preference is ~25° down from the horizontal plane. [This is correlated with an asymmetry in the horizontal recti and the monocular responses of neurons in the flocculus (see Wylie and Frost 1996 for a detailed discussion)]. With the large hand-held stimulus, the -x+z neurons prefer N-T motion in the central areas of both hemifields. As much of the receptive field of a -x+z neuron is constructed from N-T neurons in the nBOR, it is not surprising that there is a +y component to the best axes of -x+z neurons.

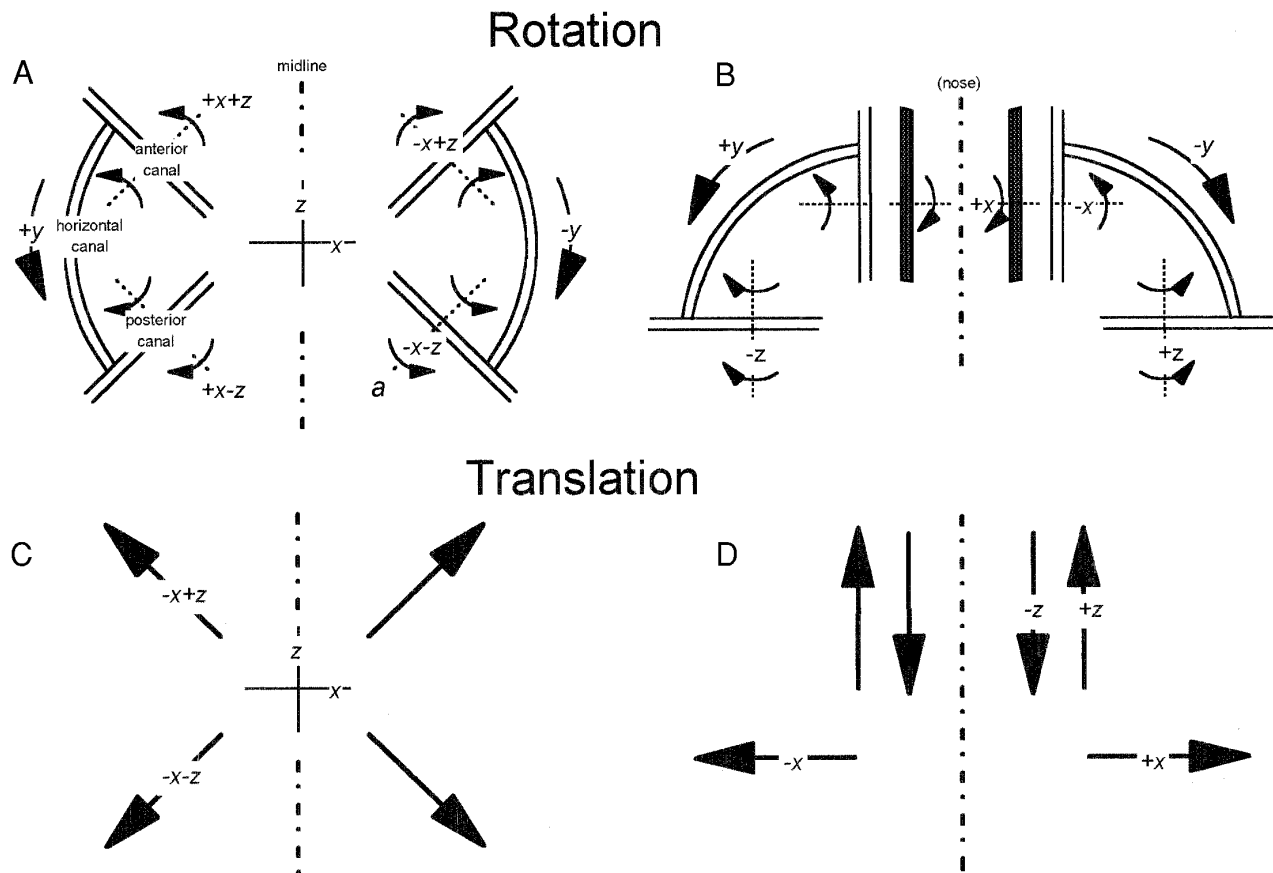


FIG. 10. Common reference frame for self-translation self-rotation. Modeled after arguments by Graf and Simpson (1985). *A*: idealized orientation of the vestibular canals of most vertebrates: a 3-axis system that fulfills the requirements of bilateral symmetry and a push-pull organization. *B*: if the system was organized such that the principal axes were the x , y , and z axes, a 4th channel is necessary. *C* and *D*: same argument holds for a self-translation system. See text for a detailed discussion.

This research was supported by grants from National Sciences and Engineering Research Council (to D.R.W. Wylie and B. J. Frost) and Alberta Heritage Foundation for Medical Research (to D.R.W. Wylie).

Address for reprint requests: D. R. Wong-Wylie, Dept. of Psychology, University of Alberta, Edmonton, Alberta T6G 2E1, Canada.

Received 15 June 1998; accepted in final form 28 September 1998.

REFERENCES

- BALDO, M. V. The spatial arrangement of the semicircular canals of the pigeon. *Braz. J. Med. Biol. Res.* 23: 914–917, 1990.
- BURNS, S. AND WALLMAN, J. Relation of single unit properties to the oculomotor function of the nucleus of the basal optic root (AOS) in chickens. *Exp. Brain Res.* 42: 171–180, 1981.
- DICKMAN, J. D. Spatial orientation of semicircular canals and afferent sensitivity vectors in pigeons. *Exp. Brain Res.* 111: 8–20, 1996.
- EZURE, K. AND GRAF, W. A quantitative analysis of the spatial organization of the vestibulo-ocular reflexes in lateral and frontal-eyed animals. I. Orientation of semicircular canals and extraocular muscles. *Neuroscience* 12: 85–93, 1984.
- FITE, K. V., BRECHA, N., KARTEN, H. J., AND HUNT, S. P. Displaced ganglion cells and the accessory optic system of the pigeon. *J. Comp. Neurol.* 195: 279–288, 1981.
- GAMLIN, P.D.R. AND COHEN, D. H. The retinal projections to the pretectum in the pigeon (*Columba livia*). *J. Comp. Neurol.* 269: 1–17, 1988.
- GIBSON, J. J. The visual perception of objective motion and subjective movement. *Psychol. Rev.* 61: 304–314, 1954.
- GIOANNI, H., REY, J., VILLALOBOS, J., AND DALBERA, A. Single unit activity in the nucleus of the basal optic root (nBOR) during optokinetic, vestibular and visuo-vestibular stimulations in the alert pigeon (*Columba livia*). *Exp. Brain Res.* 57: 49–60, 1984.
- GRAF, W. AND SIMPSON, J. I. The relations between the semicircular canals, the optic axis, and the extraocular muscle in lateral-eyed and frontal-eyed animals. In: *Progress in Oculomotor Research. Developments in Neuroscience*, edited by A. Fuchs and W. Becker. Amsterdam: Elsevier, 1981, vol. 12, p. 409–417.
- GRAF, W., SIMPSON, J. I., AND LEONARD, C. S. Spatial organization of visual messages of the rabbit's cerebellar flocculus. II. Complex and simple spike responses of Purkinje cells. *J. Neurophysiol.* 60: 2091–2121, 1988.
- HESS, B. J. AND DIERINGER, N. Spatial organization of linear vestibuloocular reflexes of the rat: responses during horizontal and vertical linear acceleration. *J. Neurophysiol.* 66: 1805–1818, 1991.
- KARTEN, H. J., FITE, K. V., AND BRECHA, N. Specific projection of displaced retinal ganglion cells upon the accessory optic system in the pigeon (*Columba livia*). *Proc. Natl. Acad. Sci. USA* 74: 1752–1756, 1977.
- KARTEN, H. J. AND HODOS, W. *A Stereotaxic Atlas of the Brain of the Pigeon (Columba Livia)*. Baltimore: Johns Hopkins Press, 1967.
- LAU, K. L., GLOVER, R. G., LINKENHOKER, B., AND WYLIE, D.R.W. Topographical organization of inferior olive cells projecting to translation and rotation zones in the vestibulocerebellum of pigeons. *Neuroscience* 85: 605–614, 1998.
- LEONARD, C. S., SIMPSON, J. I., AND GRAF, W. Spatial organization of visual messages of the rabbit's cerebellar flocculus. I. Typology of inferior olive neurons of the dorsal cap of Kooy. *J. Neurophysiol.* 60: 2073–2090, 1988.
- MACPHERSON, J. M. Strategies that simplify the control of quadrupedal stance. I. Forces at the ground. *J. Neurophysiol.* 60: 204–217, 1988.
- MORGAN, B. AND FROST, B. J. Visual response properties of neurons in the nucleus of the basal optic root of pigeons. *Exp. Brain Res.* 42: 184–188, 1981.

- REINER, A., BRECHA, N., AND KARTEN, H. J. A specific projection of retinal displaced ganglion cells to the nucleus of the basal optic root in the chicken. *Neuroscience* 4: 1679–1688, 1979.
- SI, X., ANGELAKI, D. E., AND DICKMAN, J. D. Response properties of pigeon otolith afferents to linear acceleration. *Exp. Brain Res.* 117: 242–50, 1997.
- SIMPSON, J. I. AND GRAF, W. Eye-muscle geometry and compensatory eye movements in lateral-eyed and frontal-eyed animals. *Ann. NY Acad. Sci.* 374: 20–30, 1981.
- SIMPSON, J. I. AND GRAF, W. The selection of reference frames by nature and its investigators. In: *Adaptive Mechanisms in Gaze Control: Facts and Theories*, edited A. Berthoz and G. Melvill-Jones. Amsterdam: Elsevier, 1985, p. 3–16.
- SIMPSON, J. I., GRAF, W., AND LEONARD, C. The coordinate system of visual climbing fibres to the flocculus. In: *Progress in Oculomotor Research*, edited by A. F. Fuchs and W. Becker. Amsterdam: Elsevier, 1981, p. 475–484.
- SIMPSON, J. I., GRAF, W., AND LEONARD, C. Three-dimensional representation of retinal image movement by climbing fiber activity. In: *The Olivocerebellar System in Motor Control: Experimental Brain Research Supplement*, edited by P. Strata. Heidelberg: Springer-Verlag, 1989a, vol. 17, p. 323–327.
- SIMPSON, J. I., LEONARD, C. S., AND SOODAK, R. E. The accessory optic system of rabbit. II. Spatial organization of direction selectivity. *J. Neurophysiol.* 60: 2055–2072, 1988a.
- SIMPSON, J. I., LEONARD, C. S., AND SOODAK, R. E. The accessory optic system: analyzer of self-motion. *Ann. NY Acad. Sci.* 545: 170–179, 1988b.
- SIMPSON, J. I., VAN DER STEEN, J., TAN, J., GRAF, W., AND LEONARD, C. S. Representations of ocular rotations in the cerebellar flocculus of the rabbit. In: *Progress in Brain Research*, edited by J.H.J. Allum and M. Hulliger. Amsterdam: Elsevier, 1989b, vol. 80, p. 213–223.
- VAN DER STEEN, J., SIMPSON, J. I., AND TAN, J. Functional and anatomic organization of three-dimensional eye movements in rabbit cerebellar flocculus. *J. Neurophysiol.* 72: 31–46, 1994.
- WINTERSON, B. J. AND BRAUTH, S. E. Direction-selective single units in the nucleus lentiformis mesencephali of the pigeon (*Columba livia*). *Exp. Brain Res.* 60: 215–226, 1985.
- WOLF-OBERHOLLENZER, F. AND KIRSCHFELD, K. Motion sensitivity in the nucleus of the basal optic root of the pigeon. *J. Neurophysiol.* 71: 1559–1573, 1994.
- WYLIE, D.R.W., BISCHOF, W. F., AND FROST, B. J. Common reference frame for the coding translational and rotational optic flow. *Nature* 392: 278–282, 1998.
- WYLIE, D. R. AND FROST, B. J. Visual response properties of neurons in the nucleus of the basal optic root of the pigeon: a quantitative analysis. *Exp. Brain Res.* 82: 327–336, 1990.
- WYLIE, D. R. AND FROST, B. J. Purkinje cells in the vestibulocerebellum of the pigeon respond best to either rotational or translational visual flow. *Exp. Brain Res.* 86: 229–232, 1991.
- WYLIE, D. R. AND FROST, B. J. Responses of pigeon vestibulocerebellar neurons to optokinetic stimulation. II. The 3-dimensional reference frame of rotation neurons in the flocculus. *J. Neurophysiol.* 70: 2647–2659, 1993.
- WYLIE, D.R.W. AND FROST, B. J. The pigeon optokinetic system: visual input in extraocular muscle coordinates. *Vis. Neurosci.* 13: 945–953, 1996.
- WYLIE, D.R.W. AND FROST, B. J. Responses of neurons in the nucleus of the basal optic root to translational and rotational flowfields. *J. Neurophysiol.* 81: 267–276, 1999.
- WYLIE, D. R., KRIPALANI, T.-K., AND FROST, B. J. Responses of pigeon vestibulocerebellar neurons to optokinetic stimulation. I. Functional organization of neurons discriminating between translational and rotational visual flow. *J. Neurophysiol.* 70: 2632–2646, 1993.